



PAPER

## Organic solar cells and physics education


To cite this article: Zoltán Csernovszky and Ákos Horváth 2018 *Eur. J. Phys.* **39** 045804

View the [article online](#) for updates and enhancements.

### Related content

- [Electronic and optoelectronic materials and devices inspired by nature](#)  
P Meredith, C J Bettinger, M Irimia-Vladu et al.
- [Hybrid system of semiconductor and photosynthetic protein](#)  
Younghye Kim, Seon Ae Shin, Jaehun Lee et al.
- [Roadmap on optical energy conversion](#)  
Svetlana V Boriskina, Martin A Green, Kylie Catchpole et al.

# Organic solar cells and physics education

Zoltán Csernovszky<sup>1,2</sup>  and Ákos Horváth<sup>2</sup>

<sup>1</sup> Berzsenyi Dániel Secondary School, Budapest, Hungary

<sup>2</sup> Eötvös Loránd University, Budapest, Hungary

E-mail: [csernozoli@gmail.com](mailto:csernozoli@gmail.com) and [akos@ludens.elte.hu](mailto:akos@ludens.elte.hu)

Received 2 December 2017, revised 22 February 2018

Accepted for publication 12 March 2018

Published 3 May 2018



CrossMark

## Abstract

This paper explains the operational principles of a home-made organic solar cell with the representation of an electron-cycle on an energy-level diagram. We present test data for a home-made organic solar cell which operates as a galvanic cell and current source in an electrical circuit. To determine the maximum power of the cell, the optimal current was estimated with a linear approximation. Using different light sources and dyes, the electrical properties of organic solar cells were compared. The solar cells were studied by looking at spectrophotometric data from different sensitizer dyes, generated by a do-it-yourself diffraction grating spectroscopy. The sensitizer dyes of solar cells were tested by the diffraction grating spectroscopy. The data were analysed on a light-intensity–wavelength diagram to discover which photons were absorbed and to understand the colours of the fruits containing these dyes. In terms of theoretical applications, the paper underlines the analogous nature of organic solar cells, a conventional single p–n junction solar cell and the light-dependent reactions of photosynthesis, using energy-level diagrams of electron-cycles. To conclude, a classification of photon–electron interactions in molecular systems and crystal lattices is offered, to show the importance of organic solar cells.

Supplementary material for this article is available [online](#)

Keywords: p–n junction solar cell, organic solar cell, electron-cycle, light-dependent reactions of photosynthesis, diffraction grating spectroscopy, energy levels diagram, photon–electron interaction

(Some figures may appear in colour only in the online journal)

## Introduction

The goal when using a solar cell is to transform solar energy into electrical energy. The principle behind this transformation is called the photovoltaic effect, discovered by

Edmond Becquerel in 1839. In the presence of sunlight, he measured the electrical potential difference between two platina electrodes immersed in a silver chloride solution. Because of their low output, the first solar cells were used as a power supply for satellites only, from the second half of the 20th century. The solar cells contain semiconductors, most frequently silicon, but their construction requires expensive technology. A photo-stable solar cell with lower-level technological demands was developed in the 1980s. In these cells, called dye-sensitised solar cells, or DSSCs, the absorption of solar energy is facilitated by the pigment molecules of dyes [1]. On the one hand, DSSCs have better photostability and small angular dependency, but on the other hand they have a maximum power conversion efficiency of only 12%. However, the operating principle of the DSSC paved the way for a new generation of photovoltaics, such as high-performance perovskite cells. Today, solar cells containing perovskite crystals have 22% power conversion efficiency and a very good photon–energy conversion rate. Thanks to these features, perovskite solar cells became one of the best candidates to replace high-cost conventional photovoltaics. Other emerging photovoltaics, organic solar cells, which work according to the principles of DSSCs, offer a low-cost, decorative and photovoltaic area of significant surface size for low-power solutions. A well-known example of organic photovoltaics is the Dye Solar Cell facade of the SwissTech Convention Center.

It is not only the new operating principle of the DSSCs, rather the relatively simple construction method and material demands, that draws the attention of the scientific education community; see [2–4]. During a two-year pilot project, we tested home-made organic solar cells and their dyes with 17–18 year-old secondary school students. In these circumstances, data analysis was based on secondary school mathematics. Although we used a secondary school laboratory facility, to have special semiconductor-covered glass sheets, high-temperature ovens or a professional spectrometer, we needed a university background. With the activities of this paper we can present the problem of solar energy conversion and colour vision in a real situation. The restructured energy-level representation of an electron-cycle underlines the common operational principle of solar cells and the light-dependent reactions (LDRs) of photosynthesis. Thus, organic solar cells offer an interdisciplinary application, ready to use at all levels of physics education. Preliminary results from our project have been published in [5].

## Photon–electron interactions in molecular systems and crystal lattices

In solar cells the conversion of solar energy is based on the photon–electron interaction. This type of interaction depends on two issues: the energy of the photon, and the structure where the electron is located before absorption.

In molecular systems, like green leaves, the condition necessary for solar energy to be converted into a utilisable form of energy is that the electron takes part in a chemical bond. After the interaction of the photon and the electron in the bond, the photon cuts the ( $A\bullet\bullet B$ ) chemical bond and releases the energetic radicals ( $A\bullet$ ) and ( $B\bullet$ ) (homolytic cleavage), or the whole unit seems to be excited from outside (heterolytic cleavage). In the latter case, the electrical potential, between the acceptor ( $A \cdot \cdot$ )<sup>−</sup> and donor  $D^+$  parts, can cause electrons to circulate [6].

In crystal lattices like semiconductors, the electron, which participates in conduction, jumps over the band gap from valence band (VB) to conduction band (CB) (see figure 1). Thus, an optimal solar cell has a low band gap to work on the widest possible spectrum. On the other hand, the width of the band gap indicates the stability of the solar cell. Moreover, to

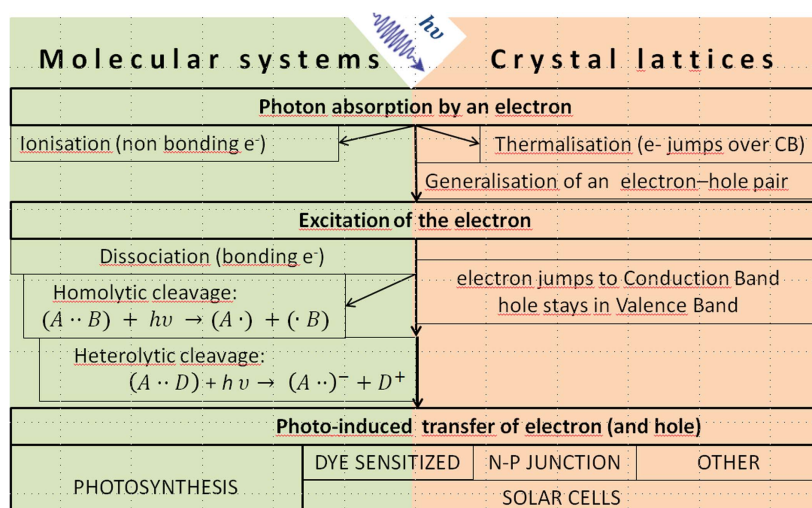


**Figure 1.** Processes where the electrons are elements of molecular systems or crystal lattices. In molecular systems after heterolytic cleavage the whole unit is excited. In crystal lattices, such as p–n junction semiconductors, the electric field of the depletion zone helps electron–hole transfer.  $(A\bullet\bullet)^-$  is an acceptor with an accepted electron;  $(D)^+$  is a donor that has passed an electron;  $\bullet$  denotes an electron.

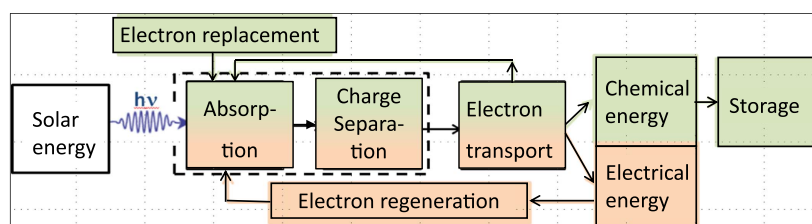


**Figure 2.** Schema of solar energy conversion in solar cells (pink) and in the LDR of photosynthesis (green).

reach higher power, a semiconductor of larger band gap is required. As a compromise, the optimum band gap for solar cells lies between 1.1 and 1.7 eV. The solution to the problem of ‘stability or efficiency’ is to divide the absorption and the charge separation functions of the depletion zone [1]. A dye helps absorption in the visible spectrum and transfers the excited electron to a semiconductor of wide band gap. Figure 2 shows an electron-cycle of solar energy conversion. Solar cells are represented in light pink, the LDR of photosynthesis in green. The broken line represents the division of the absorption and the charge separation functions in a dye-sensitised solar cell.

### A home-made organic solar cell: the raspberry solar cell

A raspberry solar cell is a DSSC cell composed of an anode glass sheet, a cathode glass sheet and an electrolyte [7]. The anode consists of transparent glass covered by a semiconductor layer (fluorine-doped tin oxide, or FTO). Onto this layer, a wide band gap semiconductor (titanium dioxide,  $\text{TiO}_2$ ) layer is fixed. Due to the nanoparticulate structure of this  $\text{TiO}_2$  layer, the size of

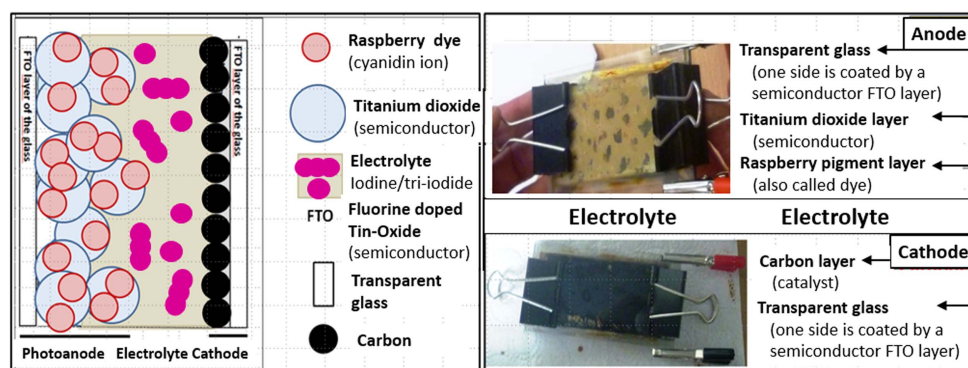


**Figure 3.** Left panel: Simplified structure of a raspberry solar cell. Right panel: A home-made raspberry solar cell. Reproduced with permission from Eotvos Lorand University and TPI-15.

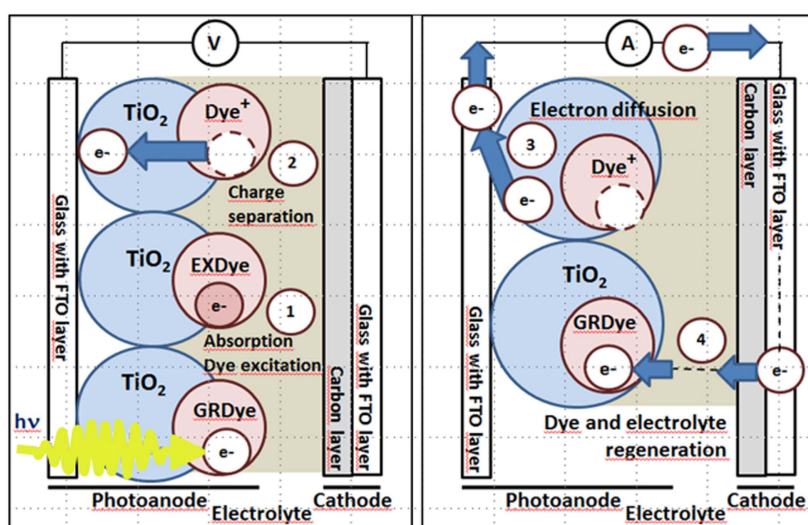


**Figure 4.** Representation of an electron-cycle in a raspberry solar cell. Steps: ① excitation of raspberry dye; ② charge separation; ③ electron diffusion to FTO glass; ④ dye and electron regenerations. Reproduced with permission from Eotvos Lorand University and TPI-15.

its final surface is of more significance than the glass sheet. It is insensitive to visible light. To prepare a light-sensitive and photostable anode, we fix light-sensitive raspberry dyes, the anthocyanin molecules, on the  $\text{TiO}_2$  layer. As a cathode, we use another transparent glass sheet with an FTO layer, covered with a graphite layer. Between these two electrodes, a regenerative iodine/tri-iodide electrolyte solution closes the circuit. See figure 3 and [4].

Due to its internal structure, the unit is a galvanic cell, and a voltage can be measured between its electrodes in the dark as well as under light irradiation. If the anode side is exposed to visible light, first a photon will be absorbed by a ground state raspberry dye molecule. The excited dye molecule injects an electron into the  $\text{TiO}_2$  crystal. Consequently, the dye and the  $\text{TiO}_2$  will be charged, because of a charge separation (see left panel of figure 4). If the two electrodes are connected on the outside using a wire, an

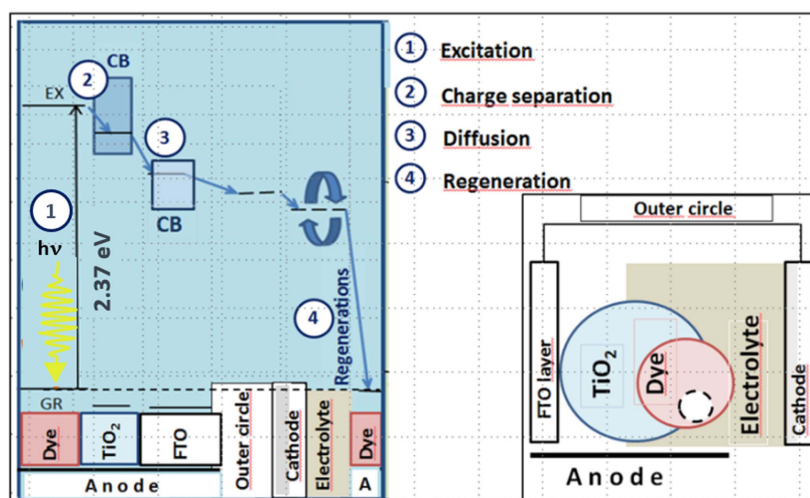


**Figure 5.** Left panel: Energy diagram and main steps in an electron-cycle in a raspberry solar cell (EX and GR are, respectively, the excited and ground state levels of dye in the CB of  $\text{TiO}_2$ ). Right panel: Physical arrangement of the components of a raspberry solar cell. Reproduced with permission from Eotvos Lorand University and TPI-15.

electric current is measurable as the electrons diffuse to the FTO layer, travel through the outer circuit, reach the cathode, and regenerate the electrolyte and dye in two steps, as shown in figure 4. See [6].

In the left panel of figure 5, we represent energy levels and bands in a raspberry solar cell. The representation follows, from left to right, the energy levels of an electron in descending order. It helps to follow an electron-cycle, even though it is different from the spatial representation. On the abscissa are the components of a raspberry cell, starting with 'Dye', which is the place of photon absorption. Figure 5, right-hand panel, shows the physical arrangement of the cell's components.

## Teaching solar cells

In practice, most solar cells use semiconductors in the form of p–n junctions. Their energy bands are deformed near the junction, where an electric field is formed. In this zone, called the depletion zone, the absorption of a photon results in an electron–hole pair. The electron jumps to the CB and the hole stays in the VB. Both the electron and the hole can participate in conduction, because the electric field in the depletion zone separates them before their recombination. See figure 6.

After diffusion to the n-type semiconductor, the electron travels through the outer circuit and will recombine with a hole, which travels in the opposite direction and diffuses to the p-type semiconductor. See the fourth panel of figure 6.

In a single p–n junction solar cell, an electron follows the same four main steps as in the raspberry solar cell: excitation, charge separation, diffusion and regeneration (see right panel of figure 7). In a raspberry solar cell, the excitation and the charge separation are spatially divided, which simplifies the description. Only the electron moves, because the positive dye ( $\text{Dye}^+$ ) is adsorbed on the  $\text{TiO}_2$  layer. These facts result in a simplified and localizable electron-cycle and energy band structure, however, the similarities are evident. See figure 7.



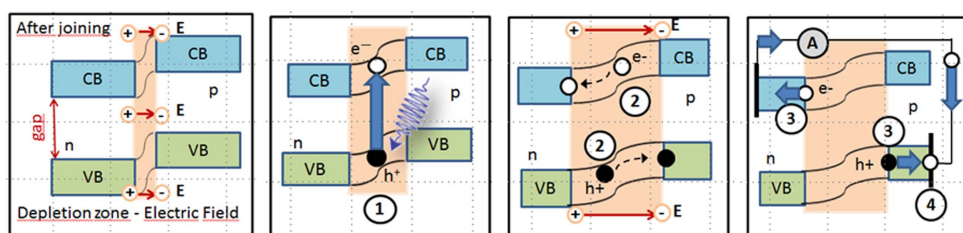


**Figure 6.** From left to right: depletion; excitation; charge separation; diffusion/regeneration.  $h^+$  = hole;  $e^-$  = electron; n/p = n-/p-type semiconductor. (From [5], reproduced with permission from Eotvos Lorand University and TPI-15).

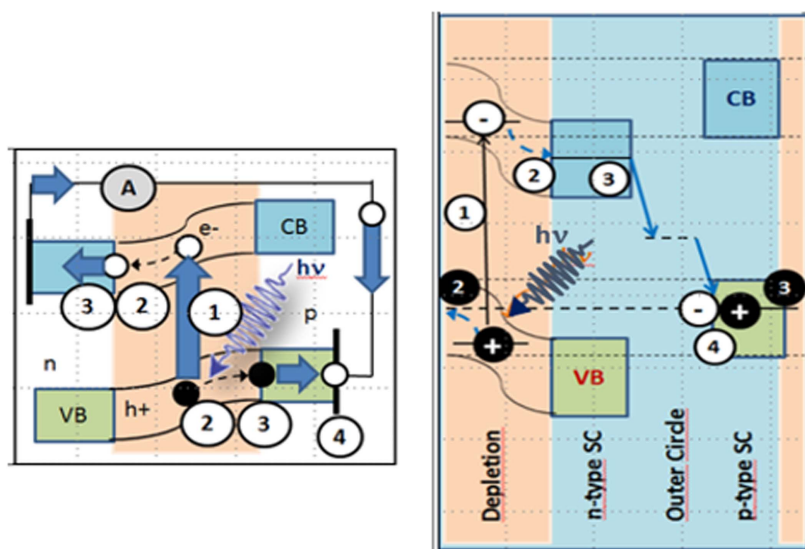


**Figure 7.** Left panel: electron/hole-cycle in a p–n junction solar cell. Right panel: Energy levels and bands of an electron-cycle ① excitation; ② charge separation; ③ diffusion; ④ regeneration; ○ electron ( $e^-$ ); ● hole ( $h^+$ ); SC = semiconductor. Reproduced with permission from Eotvos Lorand University and TPI-15.

## Teaching photosynthesis

In molecular systems like green leaves, the conversion of solar energy to chemical energy is called photosynthesis. This sequence of reactions is complex and synthesizes sugar from carbon dioxide and water using the absorbed energy of photons. The organic solar cell uses the same basic principle as plant photosynthesis to generate electricity from sunlight. Both processes require the absorption of the energy of photons. In a cycle of the LDR of photosynthesis, the electron follows the same four main steps—excitation, charge separation, diffusion and regeneration—as solar cells, but does them twice. Figure 8 shows these steps of an electron-cycle of an LDR. The absorptions of two photons of different frequencies can be seen, and that the linear electron transport chain (LETC) connects the two parts of the LDR: Photosystems I and II (PS I and PS II). The regeneration process is called photolysis (in PS II) that results in, with the electron replacement, a cyclic operation.

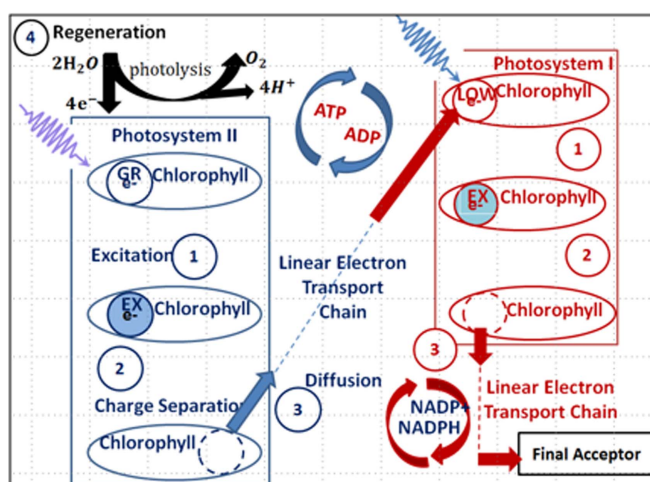


**Figure 8.** Electron-cycle of the LDR of photosynthesis: ① excitation; ② charge separation; ③ diffusion; ④ regeneration. Reproduced with permission from Eotvos Lorand University and TPI-15.

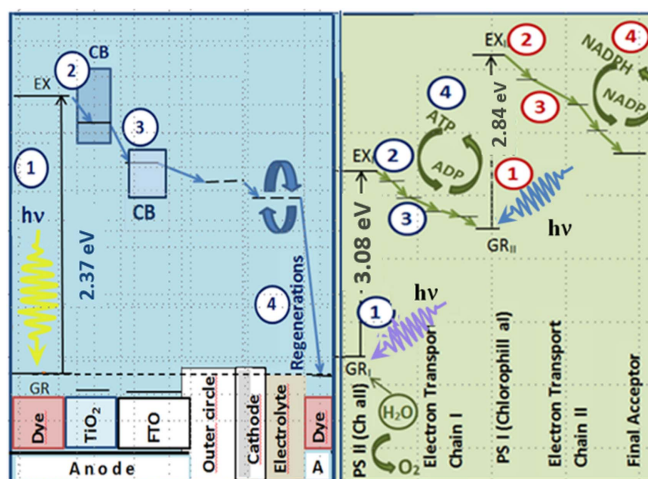


**Figure 9.** Representations of energy levels and bands of an electron-cycle. Left panel: Raspberry solar cell. Right panel: LDR. ① Excitation; ② charge separation; ③ diffusion; ④ regeneration. NADP/NADPH = nicotinamide adenine dinucleotide phosphate/oxidase molecule; ADP = adenosine diphosphate molecule; ATP = adenosine triphosphate molecule; Ch aI/aII = Chlorophyll aI/aII; EX = excited state; GR = ground state. Reproduced with permission from Eotvos Lorand University and TPI-15.

From the point of view of physics education, a comparative analysis of energy bands and levels underlines the similarities between the two processes, albeit with the electron-cycle repeated. In figure 9 the different parts of the electron-cycle of a raspberry solar cell and an LDR can be compared, along with the way they use the energy of the photons.

On the abscissa of the right panel are the components of an LDR, in spatial order, starting with the location of the photon absorption. The calculation is based on the redoxi-potential of



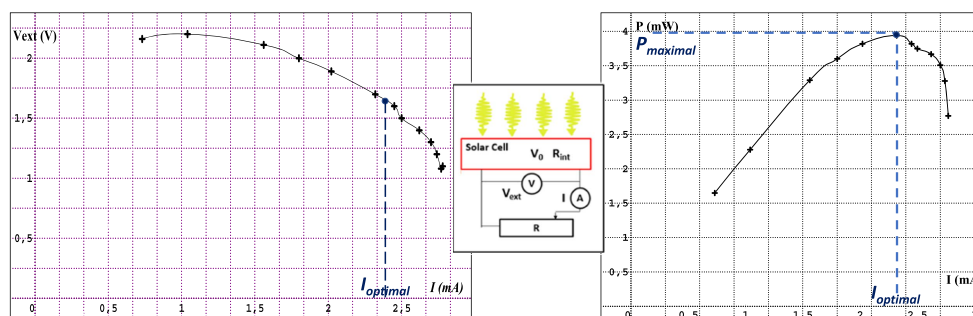


**Figure 10.** Left panel: Test results for a single p–n junction solar cell; external voltage as a function of current. Middle panel: Electrical circuit for measuring how a solar cell performs:  $\textcircled{V}$  = voltmeter;  $\textcircled{A}$  = ammeter. Right panel: Test results for a single p–n junction solar cell of power  $P$ , as a function of current.

**Table 1.** Absorption analysis of fruit and leaf extractions.

Extracts	Wavelength of absorbed photon (nm)		Energy of absorbed photon (spectrophotometer)	
	Webcam	Spectrophotometer	(eV)	( $10^{-19}$ J)
Raspberry	515	525.5	2.37	3.78
Blueberry	558	534.5	2.33	3.72
Mango	428	x	x	x
Chlorophyll a(II)	438	404	3.08	4.92
Chlorophyll b(aI)	x	438	2.84	4.54

the dioxygen/water (+0.81 V) and the final acceptor/hydrogen ion (−0.32 V) couples. In Photosystem II, when chlorophyll aII absorbs the photon its redoxi-potential passes from +0.9 V to −0.2 V [8]. We transferred the original redoxi-potential diagram to an energy-diagram, as is preferred in physics education, using the results of table 1.

### Maximal power of solar cells

In use, the current supplied by the solar cell is important, and determines the electrical power taken from it. Therefore, we applied an outer circuit where a variable resistance and a solar cell were connected (see middle panel of figure 10). We measured the external voltage ( $V_{\text{ext}}$ ) and the intensity of the current ( $I$ ) at the same time—see the results for a single p–n junction solar cell on the left- and right-hand panels of figure 10.

On the left-hand graph ( $V_{\text{ext}}-I$ ) a rapid decrease is apparent after a certain optimal current ( $I_{\text{optimal}}$ ). The power of the cell will be maximal if an optimal current is established in the circuit; see the right-hand panel of figure 10. For a detailed test of a p–n junction solar cell, see [9].

Repeating the test with a raspberry solar cell, on the one hand we measured lower voltage values, but on the other hand, on the measurable interval we found a quasi-linear relationship between voltage and current which was more easily exploitable in our secondary school project. Therefore, we used a linear regression to analyse the voltage and current data. Namely, in the left-hand panel of figure 11 we used Ohm's law in the form of

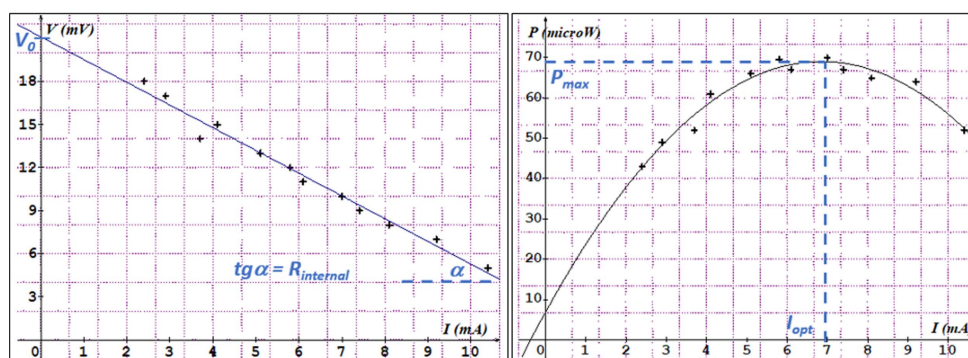


**Figure 11.** Left panel: Voltage as a function of current; interval of linear dependence. Right panel: Power as a function of current, showing maximal power and optimal current. Reproduced with permission from Eotvos Lorand University and TPI-15.

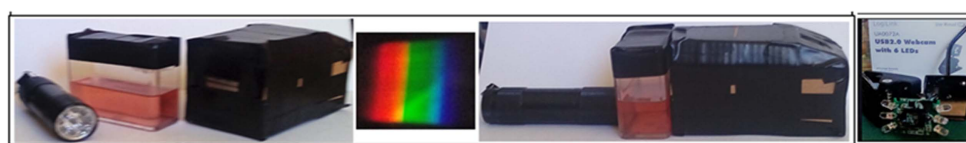


**Figure 12.** Light source, raspberry extraction and diffraction grating spectroscope; spectrum; experimental setup; webcam as a USB-spectrometer.

$V_{\text{ext}} = V_0 - R_{\text{int}} \cdot I$  where  $R_{\text{int}}$  is the internal resistance (gradient of the line  $V_{\text{ext}}(I)$ ) and  $V_0$  is the electromotive force of the cell (intersection of the line  $V_{\text{ext}}(I)$  and the  $V$ -axis). We find  $V_{\text{ext}}$ , and then we can calculate the optimal current value  $I_{\text{optimal}} = \frac{V_0}{2 \cdot R_{\text{int}}}$  and the maximal power of the raspberry solar cell  $P_{\text{optimal}} = \frac{V_0^2}{4 \cdot R_{\text{int}}}$ .

Another possibility for finding the optimal current is to analyse the  $P-I$  relationship of the linear regression (see figure 11, right panel), and find the maximum power value of the second order approximation as the maximum of parabola  $P(I)$ .

## Absorption properties of some organic dyes

To examine the absorption properties of organic dyes and chlorophylls, we prepared pigment extractions with 5.5 g crushed fresh fruits and 95 ml methanol. After filtration, we added 1 ml hydrochloric acid to the solutions, and the extractions were exposed to candlelight. It is possible to construct a low-cost diffraction grating spectroscope using a CD, and then analyse the spectra using a webcam and data analysis software [10, 11], figure 12.

From [11], the spectroscope has a single slit made from two parallel razor blades, and a CD placed as shown in the left panel of figure 13. The disc reflects and diffracts the incident beam, because it operates as both a mirror and a diffraction grating. See figure 13, left panel, to follow the path of a ray of wavelength  $\lambda$ , between its source and the webcam. To determine the direction of a first order diffracted ray (the most convenient ray for analysis), we measured  $\alpha_1 \approx 22^\circ$  with a helium–neon laser (LD Didaktik,  $\lambda = 632.8 \text{ nm}$ ). See figure 13, right panel. It is measured starting from the reflected ray.

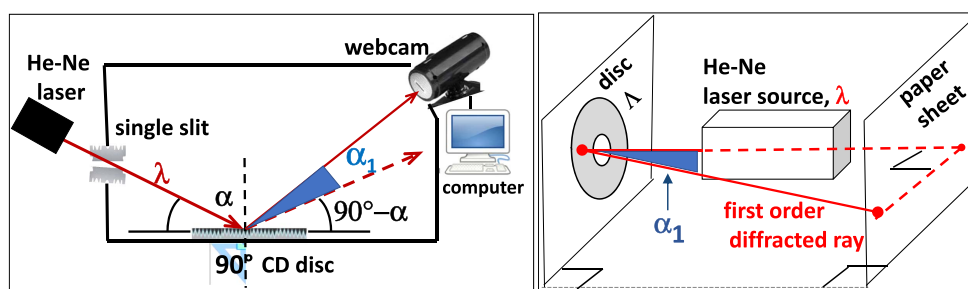


**Figure 13.** Left panel: DIY diffraction grating spectroscopy; first order diffracted ray of wavelength  $\lambda$ . Right panel: How to determine the direction of first order diffracted rays ( $\alpha_1$ ).

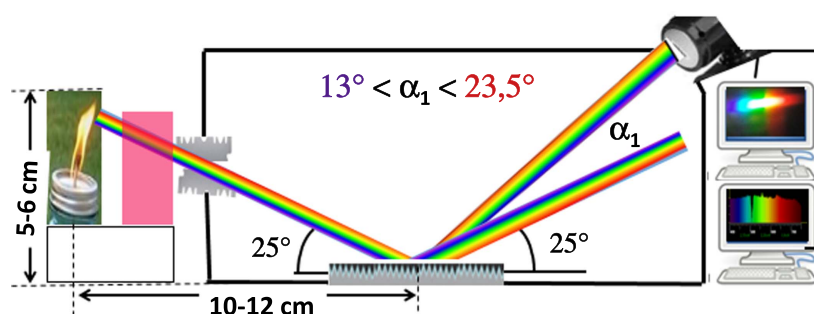


**Figure 14.** How to determine the direction of the webcam (spectral image of candlelight traversing an extract).

Use an anti-repellent candle to create a flame of height 3–4 cm. Place an extract between the candle and the slit, then fix the spectroscopy as shown in figure 14. To find a convenient direction for the webcam, first we calculate the spacing of grooves on the disc ( $\Lambda$ ). This latter determines the first order diffraction direction of a ray of wavelength  $\lambda$  with the relation:  $\sin \alpha_1 = \lambda / \Lambda$ . With laser data as above, we have  $\Lambda_{CD} = \lambda / \sin \alpha_1 = 1750 \text{ nm}$ . For a compound light,  $\lambda$  is between 400 and 700 nm, thus  $\alpha_1$  is between  $13^\circ$  (purple) and  $23.5^\circ$  (red).

If we focus the first order diffracted and reflected beam on the charge-coupled device of the webcam, carry out a calibration and connect the camera to a computer equipped with data analysis software such as *Tracker* or *sp2012* (see [10] and [11] for more detail), the software calculates the incident light intensity depending on wavelength, or photon energy. We found dark lines on the diagrams, indicated in figure 15 with white arrows and approximate wavelength values. These wavelengths are associated with the photons absorbed by the extracts placed between candle and slit.

These absorption analysis results were compared to results obtained by a PerkinElmer Lambda 35 UV–vis spectrometer, see figure 16. We determined the absorbed photon energy ( $E$ ) using the Planck formula  $E = h\nu$ , where  $h$  is the Planck constant and  $\nu$  is the frequency of the absorbed photon (see table 1). We used these determined energy values of absorbed photons in figures 5, 7 and 9.

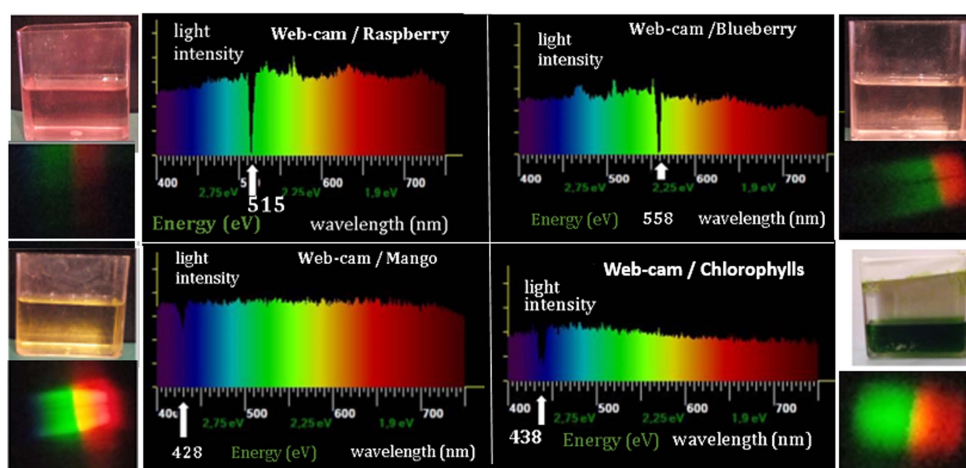


**Figure 15.** Spectra of extracts exposed to candlelight, produced by a DIY spectroscope, and analysed by webcam.

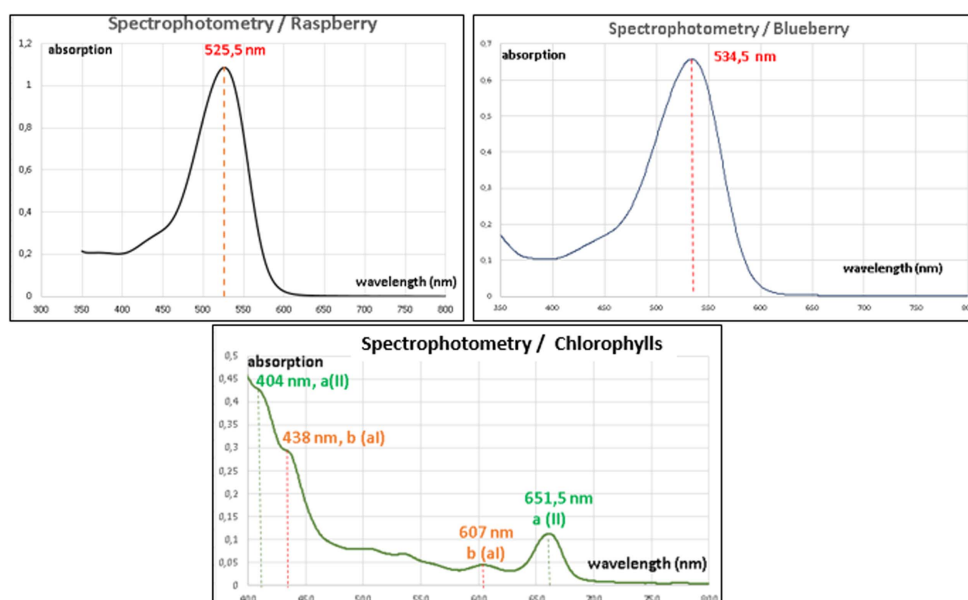


**Figure 16.** Spectrophotometry results: absorption of different extracts as a function of wavelength, with the wavelengths of absorption maxima shown.

The colours of berries (and of fruits and leaves more generally) on a molecular level depend on the chromophore and auxochrome groups of their anthocyanidin molecules. To be coloured, the molecule must have regularly alternating double and single bonds, plus double bonds must be in conjugated positions. Figure 22 shows examples.

It is characteristic of an anthocyanin ion that the chromophore group determines primarily the wavelength of the absorbed photon, and the auxochrome group can modify it by shifting to higher values. Figure 22 compares the similar structures of raspberry and

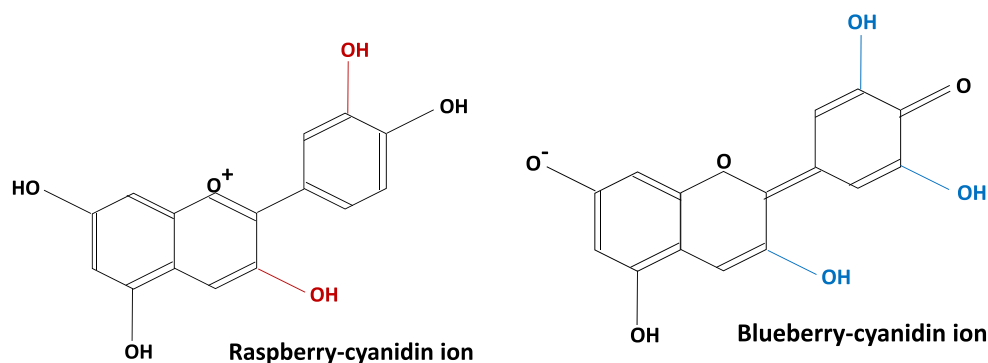


**Figure 17.** Raspberry- and blueberry-cyanidin ions. Chromophore (black) and auxochrome groups (coloured).

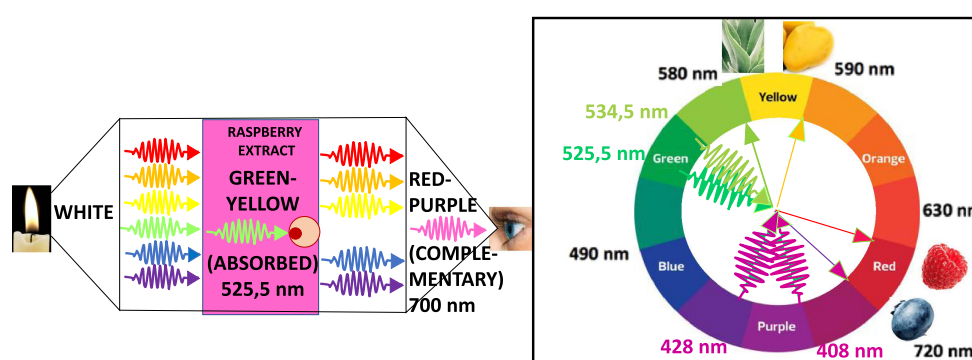


**Figure 18.** Absorption and colour: mechanism (left) and colour wheel (right).

blueberry-cyanidin ions, and so we can understand their similar colours and the close values of the absorption maxima wavelengths: 525.5 nm and 534.5 nm respectively (see figure 16).

The mechanism of colour vision is based on the fact that the absorbed colour is missing from the colour seen (see left-hand panel of figure 17). In the case of raspberry extract, the green–yellow colour is absorbed, and so the colour seen is the sum of the non-absorbed colours, the red–purple. We can quickly determine the complementary colours, in other words the colours of fruits and leaves, using the colour wheel of figure 17, right panel. The colour of the fruit or leaf is on the opposite side of the colour wheel to the absorbed photon.

### Organic solar cells as voltaic source

To test the constructed raspberry solar cell, we measured the voltage between the electrodes in the dark, and then again after the cell had been exposed to a neon- and to an LED light source. See figure 18.

Using raspberry, blueberry and mango extracts we constructed other organic solar cells, too. We exposed these cells to different light sources (LED, reflector, UV, bulb and halogen) to measure the voltages between electrodes. See figure 19, right panel.

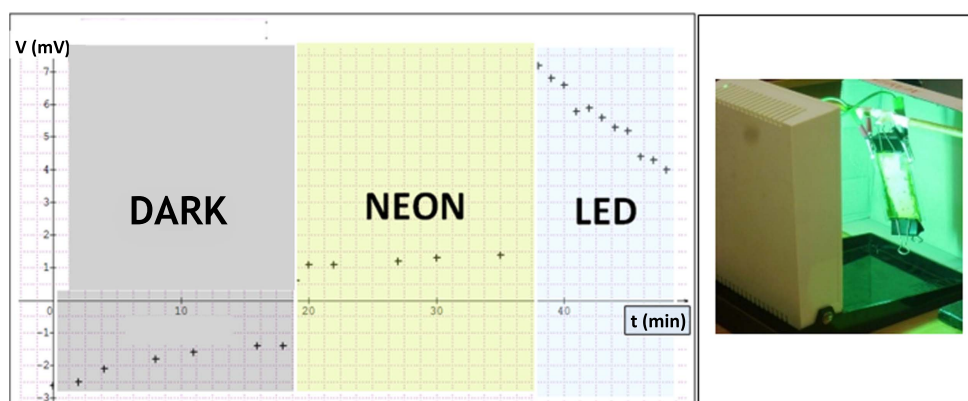


**Figure 19.** Left panel: Voltage measured between the electrodes of a raspberry solar cell exposed to different light sources, as a function of time. Right panel: Raspberry solar cell being exposed to neon light.

The raspberry solar cell (red line) reacts to different sources in the same way as the blueberry solar cell (blue line) does, but the measured voltages were a little higher for the raspberry than for the blueberry. We found that the mango solar cell (yellow line) was not as sensitive to light sources as the two other solar cells. All three of the solar cells are the most sensitive to the UV light source. We think that the weak mango dye adsorption to the  $\text{TiO}_2$  layer can result in extreme voltage responses, including 0 V. For this reason, we recommend using raspberry or blueberry dyes to construct more stable organic solar cells. We underline here that these voltage values are relative values which express average quotients of the voltage responses of the cells.

During analysis of the correlations between light sources' emission spectra, organic dyes' absorption spectra, and voltage responses, we considered whether the measured values were sensitive to the incident light intensity and to the construction method used. We found correlations in the case of a mercury-vapour UV lamp (see figure 20). The peaks in the emission spectrum and the dyes' absorption maxima are matched. Namely, the blue–violet emission peak matches the mango absorption maxima, and the green–yellow peak matches those of raspberry and blueberry. The difference in emission spectrum intensity peaks can explain the voltage difference between organic solar cells.

In the case of the LED and the reflector, the mango voltage comes from the yellow–red part of the emission spectrum. Regarding the reduced voltage responses of the raspberry and blueberry solar cells, we explain these by the reduced peak intensity in the emission spectra, due to the spectra being more steady (figure 21, upper panels). With the bulb, the weak voltage responses are due to steady, but more intensive, red components of the spectrum. In the halogen case, we add to this argument that the weak peaks of the emission spectrum are different to the absorption spectra maxima of the dyes. See figure 21, lower panels.

In these organic solar cells, the electrical properties are based largely on sensitizers. In an ideal case, a photostable sensitizer is adsorbed strongly to the  $\text{TiO}_2$  layer such that it has a wide absorption spectrum, and the absorbed photon excites the dye and efficiently injects the excited electron into the CB of the  $\text{TiO}_2$ . The quality of the sensitizer is determined by the anthocyanidin molecule of the dye. See figure 22 and [12].



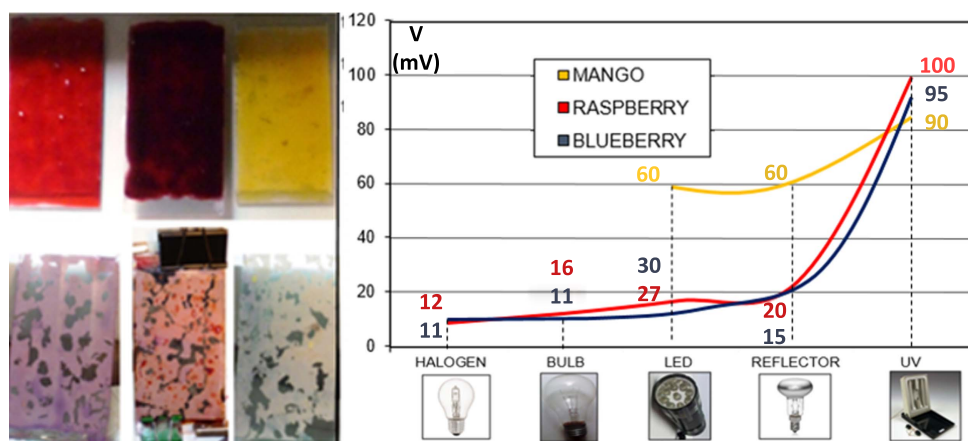


**Figure 20.** Left panel: Raspberry, blueberry and mango extracts and anodes. Right panel: Different light sources and corresponding voltages for raspberry, blueberry and mango solar cells.

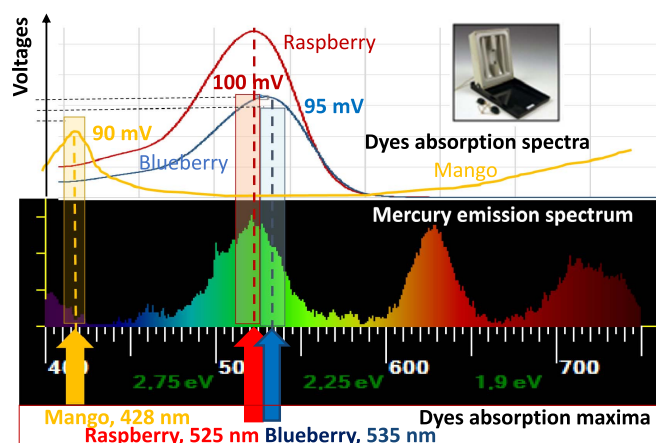


**Figure 21.** Mercury-vapour lamp emission spectrum, dyes' absorption maxima and voltages of organic solar cells (see also figure 16 and table 1).

## Conclusions

This paper proposes the construction of organic solar cells, although the do-it-yourself method is recommended only for students over 17 years old, with detailed instructions, a teacher to assist them, and in a laboratory setting. The activities described aim to illustrate the versatility of organic solar cells. If we organise the concept of energy around activities realised by organic solar cells, the students can integrate many pre-existing concepts using their own experiences, and by analysing their own data.

To place the topic in an interdisciplinary context, with a relatively simple electron-cycle and energy band structure the organic solar cell can help establish an understanding of the more complex p–n junction solar cell and of LDRs in photosynthesis. Based on these similarities, we built up a simplified model to underline the basic common principle. Electron-

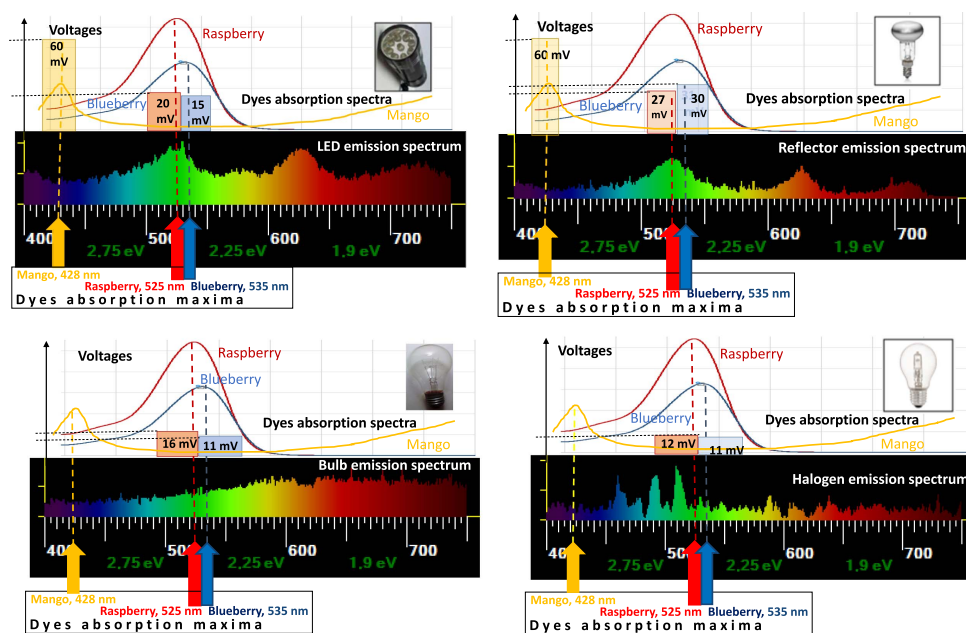


**Figure 22.** Emission spectra of different light sources (top: LED, reflector; bottom: bulb, halogen lamp). Absorption spectra of mango, raspberry and blueberry dyes—voltages of these organic solar cells.

cycle and energy-level analogies can help describe all types of solar energy converters, and many issues of environmental sciences.

## Acknowledgments

This study was funded by the Content Pedagogy Research Program of the Hungarian Academy of Sciences. Special thanks to Gábor Vass for cooperation on the topic of spectrophotometry.

## ORCID iDs

Csernovszky Zoltán  <https://orcid.org/0000-0002-2097-6233>

## References

- [1] Smestad G P and Grätzel M 1998 Demonstrating electron transfer and nanotechnology: a natural dye-sensitized nanocrystalline energy converter *J. Chem. Educ.* **75** 752–6
- [2] Appleyard S J 2006 Simple photovoltaic cells for exploring solar energy concepts *Phys. Educ.* **41** 409
- [3] Appleyard S J 2008 Experimenting with photoelectrochemical cells in drinking straws *Phys. Educ.* **43** 270
- [4] Ireson G *et al* 2006 Solar energy revisited: creating and using Grätzel cells at school *Phys. Educ.* **41** 377

- [5] Csernovszky Z and Horváth A 2017 Raspberry solar cell, a versatile tool in teaching physics *Int. Conf. Teaching Physics Innovatively* ed T Tél and A Király (Budapest: Graduate Sch. for Physics, Eötvös Univ.) pp 149–54
- [6] Le Bahers T 2011 Optimisation des cellules solaires a colorants a base de ZnO par une approche combinée théorie/expérience *These de doctorat* de l'Université Pierre et Marie Curie, Paris VI
- [7] O'Regan B and Grätzel M 1991 A low-cost, high-efficiency solar cell based on dye-sensitized colloidal TiO<sub>2</sub> films *Nature* **353** 737–40
- [8] Tavernier R 1989 *Biologie Terminale D* (Paris: Édition Bordas) Collection Tavernier, Édition Bordas, (p.131, figure 2)
- [9] Zachariadou K *et al* 2012 A low-cost computer-controlled Arduino-based educational laboratory system for teaching the fundamentals of photovoltaic cells *Eur. J. Phys.* **33** 1599
- [10] Rodrigues M *et al* 2016 How to build a low cost spectrometer with Tracker for teaching light spectra *Phys. Educ.* **51** 014002
- [11] Piláth K 2012 The matching of a jointly used diffraction grating spectroscope and a web camera *Fizikai Szemle* **692** 126–7
- [12] Etula J 2012 Comparison of three Finnish berries as sensitizers in a dye-sensitized solar cell *Eur. J. Young Sci. Eng.* **1** 5–23